

To be published in Journal of the Optical Society of America B:

Title: Metamaterial Absorber with Dendritic cells at Infrared Frequencies

Authors: Wei Zhu and Xiao Zhao

Accepted: 22 October 2009

Posted: 26 October 2009

Doc. ID: 111709



Metamaterial Absorber with Dendritic cells at Infrared Frequencies

Weiren Zhu, Xiaopeng Zhao*

Smart Materials Laboratory, Department of Applied Physics, Northwestern
Polytechnical University, Xi' an 710072, P.R.China

*Corresponding author: E-mail: xpzhao@nwpu.edu.cn

We present the model of infrared metamaterial absorber composed of metal dendritic resonators, dielectric substrate, and continuous metal film. Numerical simulation confirms an absorptivity of 98.6% at the infrared wavelength of $2.79\mu\text{m}$. The proposed metamaterial absorber has an excellence of two-dimension isotropy, and it could be fabricated with a chemical double template technique. Our simulation shows it could be operated for a wide range of incident angle. The optical metamaterial absorber proposed in this paper has potential applications such as infrared imaging device, thermal bolometers, and wavelength-selective radiator.

OCIS codes: (160.4670) Optical materials; (160.3918) Metamaterials.

Over the past several years, artificial engineered electromagnetic (EM) metamaterials have received a great deal of interest [1,2]. The basic idea of metamaterials is geometrically design the artificial “atoms” to create electric [3] and/or magnetic [4] response to the incident EM radiation, which results in arbitrarily controllable electric permittivity $\varepsilon=\varepsilon_1+i\varepsilon_2$ and magnetic permeability $\mu=\mu_1+i\mu_2$. The realization of left-handed materials with negative ε_1 and negative μ_1 simultaneously was confirmed by Shelby [2] in 2001, greatly accelerating the research of metamaterials. Since that, various metallic artificial structures, such as S-shaped resonators [5,6], paired nanorods [7], dendritic cells [8,9], and double fishnet structure [10,11], have been proposed in pursuing the negative refraction or negative magnetic response. The EM invisibility cloaks of transformation optics are also based on the design of metamaterials [12].

Quite recently, Landy *et al.* [13] demonstrated that the metamaterial could be designed as EM absorber, and confirmed the almost complete absorption at microwave frequencies. Compared to the electromagnetic absorber designed with frequency selective surface (FSS), which is a periodic effect of metal array and the unit cell size is comparable to the wavelength [14], the high absorptivity of the metamaterial absorber are mainly due to the local electromagnetic resonance, and the unit cell is smaller than the wavelength in accordance with the effective medium theory. With the similar design, Tao *et al.* [15] subsequently reported an absorptivity of 70% at 1.3 terahertz experimentally. Later, Tao *et al.* [16] presented a metamaterial absorber with polarization-insensitive at THz frequency. Avitzour [17] reported a

wide-angle infrared absorber based on a negative-index plasmonic metamaterial. However, the actualization of optical metamaterial absorber remains as a great challenge, which mainly depends on preparing appropriate metamaterial operated at optical frequencies. Although the fishnet structure [11] or paired nanorods [7] has already reported as optical metamaterial, the complexity, inefficient and costliness of physical lithography still come to be the obstacle of the further developing.

In our previous studies, Liu *et al.* [18] presented the dendritic metamaterial at infrared frequency with a chemical double template technique, which provides a facile, low-cost way to fabricate metamaterial of larger areas at infrared and even visible frequencies. In this paper, we show the infrared metamaterial absorber can be achieved with a sandwich model composed of metal dendritic resonators, dielectric substrate, and continuous metal film. This structure could be fabricated conveniently as the similar method in Ref. [18]. Besides, the proposed metamaterial absorber has an excellence of two-dimension isotropy, and it could be operated for a wide range of incident angle. The proposed metamaterial absorber may have potential applications in electromagnetics and optics, such as infrared imaging device, thermal bolometers, and wavelength-selective radiator.

Figure 1 shows the single unit cell of our dendritic metamaterial absorber. For EM wave normal incidence, the symmetrical dendritic resonator acts as an electric-LC resonator [19], supplying the electric coupling to incident E field. The magnetic coupling is created by the antiparallel currents between the dendritic cell and metal film response to the incident H field. For appropriately modulating the

geometrical parameters, the electric and magnetic resonances can be well overlapped in the given frequency range, providing the ability to absorb the electric and magnetic energy almost completely.

Here, we first give a microwave example of this metal-dielectric-metal sandwich model. The metal is chosen as copper with the thickness of 0.017mm, and the dielectric substrate is 0.8mm thick epoxy glass. The geometry dimension parameters are as follows: $a=1.8\text{mm}$, $b=0.8\text{mm}$, $c=0.7\text{mm}$, $\theta=45^\circ$, $w=0.3\text{mm}$. The lattice constant d of the sample is equal to 10mm in both the E direction and the H direction. Using a shadow mask/etching technique, the experimental sample is fabricated with 12 units in both E and H direction.

The numerical simulations are taken by a Germany commercial software package CST Microwave Studio, which is based on finite integration method. In our simulations, the copper is set as lossy metal, and the electric conductivity is 5.8×10^7 S/m. The permittivity of the epoxy glass substrate is 4.6 with the loss tangent of 0.025.

For plane EM wave normal incidence, there is no transmission field able to be measured, as is blocked off by the metal film. Thus, only the reflectance needs to be concerned in our simulations and experiments.

In fig. 2(a), we show the S_{11} (the amplitude of reflection) from simulation and measurement in comparison with each other. There are obvious dips appeared near the frequency of 10.26GHz in both the curves, and the dip value is $S_{11}=0.024$ in simulation and $S_{11}=0.212$ in experiment. The absorptivity can be described as

$A(\omega)=1-S_{11}^2$, and fig. 2(b) shows the absorptivity calculated from simulation and experiment. Close to the frequency of 10.26GHz, the absorptivity of 99.9% in simulation and 95.5% in experiment are achieved, quite in accordance with each other, which shows the very good absorption characteristic.

If the dimensions of the dendritic structure are reduced down to nano scale, our structure will give perfect absorption at optical frequency. Ref. [18] shows the infrared dendritic metamaterial prepared with a chemical double template technique. Our metamaterial absorber could be prepared with the similar method that combines with a thin silver film. Here, we give a simulation example of the metamaterial absorber that work at infrared frequency. The geometry dimension parameters are as follows: $a=90\text{nm}$, $b=52.5\text{nm}$, $c=45\text{nm}$, $\theta=45^\circ$, $w=22.5\text{nm}$. The dielectric medium is 40nm-thick SiO_2 , and is treated as no loss substrate with the electric permittivity of 2.25. The metal is chosen as Ag, and the thickness of dendritic pattern and the continuous film is 25nm and 50nm, respectively. In our simulation, the free electron Drude model with plasma frequency $\omega_p=1.37\times 10^{16}\text{s}^{-1}$ and collision frequency $\omega_c=8.5\times 10^{13}\text{s}^{-1}$ is adopted to characterize the permittivity for Ag. The lattice constant d of the sample is equal to 700nm in both the E direction and the H direction.

Figure 3 shows the S parameters and absorptivity of this structure. It is found that the S_{11} has a sudden dip near the wavelength of $2.79\mu\text{m}$ (107.5THz), the minimum of which is 0.051. The S_{21} (the amplitude of transmission) is quite small at the whole wavelength reign, and get 0.105 at $2.79\mu\text{m}$. The absorptivity could be calculated as $A(\omega)=1-S_{11}^2-S_{21}^2$, and as high as 98.6% is achieved for our model. The result shows

clearly the viability of using silver dendritic cells to build metamaterial absorber at infrared frequencies, if combines with additional continuous silver film. Our next aim is to experimentally actualize the optical metamaterial absorber based on dendritic cells with the chemical double template technique.

To better understand its observed performance, we examined the current density distribution of the metamaterial absorber at the resonance wavelength of $2.79\mu\text{m}$ (fig. 4). For EM wave normal incidence, the current density in the metal dendritic cell is symmetrical, which is similar as the electric-LC resonator [19], and provides the electric response. It can be seen that, the current density in the metal film is concentrated strongly face to face with the dendritic cell, and is anti-parallel with that in the dendritic cell, which is similar to the so-called fishnet [11] or paired nanorod structures [7], providing the magnetic response. The current density distribution is quite in accordance with the anticipation above, and the electric response and magnetic response appear simultaneously at the given wavelength.

Figure 5 shows the simulated absorption of our metamaterial absorber at various angles of oblique incidence for TE and TM radiation. It could be found that, for TE case [fig 5(a)], the peak absorptivity of 98.6% is obtained at normal incidence. With increasing angle of incidence, there is a monotonic decrease in the absorptivity. However, the absorptivity remains higher than 94.8% for incident angle smaller than 45° . Beyond 60° , there is a sudden decrease in the absorptivity. This could be explained as the fact that, with the increase of incidence angle, the incident magnetic flux between the Ag dendritic cell and Ag film comes to be less and less. It is

therefore less effective to drive a strong magnetic resonance. Thus, only the electric resonance is dominant, and most of the EM energy of the incident wave is reflected back caused by the intense impedance mismatch. For the case of TM radiation [fig 5(b)], the absorption remains greater than 98% for all angles of incidence. In this case, the magnetic flux is effective to provide the strong magnetic resonance at all angles of incidence, which is important to maintain impedance matching. Our simulated result shows this metamaterial absorber could be worked at a wide range of incident angles, which is similar to the polarization-insensitive THz metamaterial absorber reported in [17]. The availability of wide angles incidence is quite a useful performance for applications such as infrared imaging, and thermal bolometers.

In conclusion, we present a sandwich model of metamaterial absorber composed of metal dendritic resonators, dielectric substrate, and continuous metal film. Microwave experiments confirm an absorptivity of 95.5% at the frequency of 10.26GHz. This model could be prepared at optical frequencies with a chemical template technique, and our simulation shows an absorptivity of 98.6% at infrared wavelength of 2.79 μ m. The current densities are analyzed to understand the resonance mechanism. Our dendritic metamaterial absorber has an excellence of two-dimension isotropy, and the simulation shows it could be operated for a wide range of incident angles. The optical metamaterial absorber proposed in this paper has potential applications such as infrared imaging device, thermal bolometers, and wavelength-selective radiator.

We acknowledge support from the National Natural Science Foundation of

China under Grant No. 50632030, 50872113, 50936002.

Published by

OSA

References

1. V. G. Vesalago, "Electrodynamics of substances with simultaneously negative values of ϵ and μ ," *Sov. Phys. Usp.* **10**, 509-514 (1968)
2. R. A. Shelby, D. R. Smith, and S. Schultz, "Experimental Verification of a Negative Index of Refraction," *Science* **292**, 77-79 (2001)
3. J. B. Pendry, A. J. Holden, W. J. Stewart, and I. Youngs, "Extremely Low Frequency Plasmons in Metallic Mesostructures," *Phys. Rev. Lett.* **76**, 4773-4776 (1996)
4. J. B. Pendry, A. J. Holden, D. J. Robbins, and W. J. Stewart, "Magnetism from Conductors and Enhanced Nonlinear Phenomena," *IEEE Trans. Microwave Theory Tech.* **47**, 2075-2084 (1999)
5. H. S. Chen, L. X. Ran, J. T. Huangfu, X. M. Zhang, K. S. Chen, T. M. Grzegorzczuk, and J. A. Kong, "Left-handed materials composed of only S-shaped resonators," *Phys. Rev. E* **70**, 057605 (2004)
6. H. S. Chen, L. X. Ran, J. T. Huangfu, X. M. Zhang, K. S. Chen, T. M. Grzegorzczuk, and J. A. Kong, "Negative refraction of a combined double S-shaped metamaterial," *Appl. Phys. Lett.* **86**, 151909 (2005)
7. V. M. Shalaev, W. Cai, U. K. Chettiar, H. K. Yuan, A. K. Sarychev, V. P. Drachev, and A. V. Kildishev, "Negative index of refraction in optical metamaterials," *Opt. Lett.* **30**, 3356-3358 (2005)
8. X. Zhou and X. P. Zhao, "Resonant condition of unitary dendritic structure with overlapping negative permittivity and permeability," *Appl. Phys. Lett.* **91**, 181908 (2007).

9. W. R. Zhu, X. P. Zhao, and J. Q. Guo, "Multibands of negative refractive indexes in the left-handed metamaterials with multiple dendritic structures," *Appl. Phys. Lett.* **92**, 241116 (2008)
10. M. Kafesaki, I. Tsiapa, N. Katsarakis, Th. Koschny, C. M. Soukoulis, and E. N. Economou, "Left-handed metamaterials: The fishnet structure and its variations," *Phys. Rev. B* **75**, 235114 (2007)
11. G. Dolling, M. Wegener, C. M. Soukoulis, S. Linden, "Negative-index metamaterial at 780 nm wavelength," *Opt. Lett.* **32**, 53-55 (2007)
12. D. Schurig, J. J. Mock, B. J. Justice, S. A. Cummer, J. B. Pendry, A. F. Starr, and D. R. Smith, "Metamaterial Electromagnetic Cloak at Microwave Frequencies," *Science* **314**, 977-980 (2006).
13. N. I. Landy, S. Sajuyigbe, J. J. Mock, D. R. Smith, and W. J. Padilla, "Perfect Metamaterial Absorber," *Phys. Rev. Lett.* **100**, 207402 (2008)
14. D. J. Kern and D. H. Werner, "A genetic algorithm approach to the design of ultra-thin electromagnetic bandgap absorbers," *Microw. Opt. Techn. Lett.* **38**, 61-64 (2003)
15. H. Tao, N. I. Landy, C. M. Bingham, X. Zhang, R. D. Averitt, and W. J. Padilla, "A metamaterial absorber for the terahertz regime: Design, fabrication and characterization," *Opt. Express* **16**, 7181-7188 (2008)
16. H. Tao, C. M. Bingham, A. C. Strikwerda, D. Pilon, D. Shrekenhamer, N. I. Landy, K. Fan, X. Zhang, W. J. Padilla, and R. D. Averitt, "Highly flexible wide angle of incidence terahertz metamaterial absorber: Design, fabrication, and characterization," *Phys. Rev. B* **78**, 241103(R) (2008)

17. Y. Avitzour, Y. A. Urzhumov, and G. Shvets, "Wide-angle infrared absorber based on a negative-index plasmonic metamaterial," *Phys. Rev. B* **79**, 045131 (2009)
18. H. Liu, X. P. Zhao, Y. Yang, Q. W. Li, and J. Lv, "Fabrication of Infrared Left-Handed Metamaterials via Double Template-Assisted Electrochemical Deposition," *Adv. Mater.* **20**, 2050-2054 (2008)
19. D. Schurig, J. J. Mock, and D. R. Smith, "Electric-field-coupled resonators for negative permittivity metamaterials," *Appl. Phys. Lett.* **88**, 041109 (2006)

Published by

OSA

Figure captions

Fig.1. (Color online) Scheme of single unit cell of the metamaterial absorber (left), the geometrical parameters are defined as show in right.

Fig.2. (Color online) The S_{11} (a) and absorptivity (b) from simulations and microwave experiments.

Fig.3. (Color online) The S parameter and absorptivity of the infrared metamaterial absorber from simulations.

Fig.4. (Color online) The current density distribution for the metamaterial absorber at the wavelength of $2.79\mu\text{m}$.

Fig.5. (Color online) Angular dependence of the absorptivity of the metamaterial absorber for TE incidence (a) and TM incidence (b).

Figures

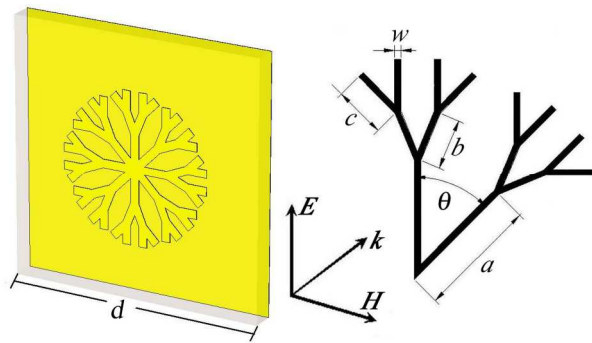


Fig 1

Published by

OSA

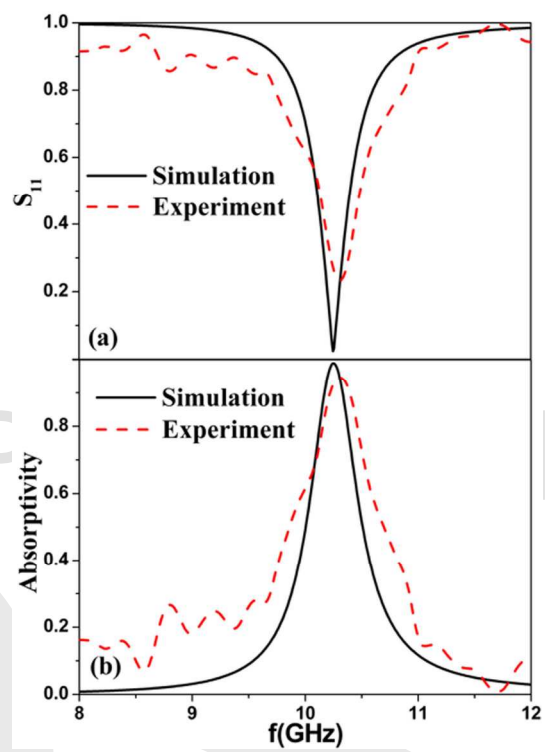
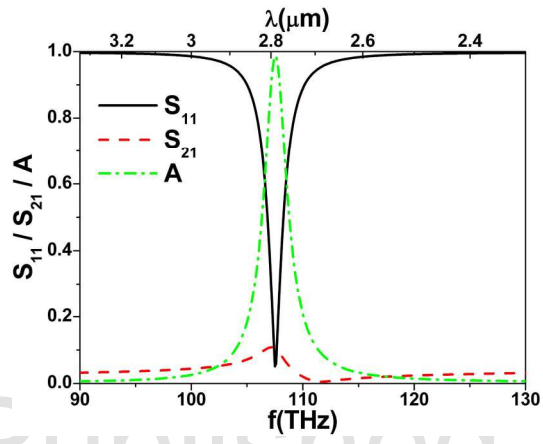


Fig 2



Furnished by

OSA

Fig 3

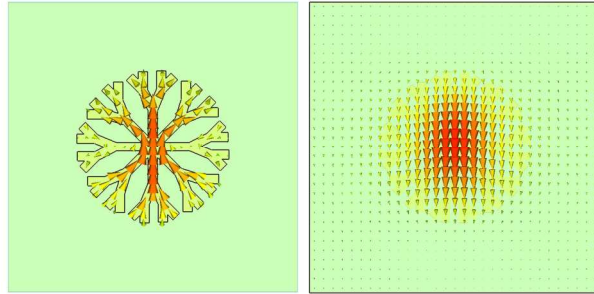


Fig 4

Published by

OSA

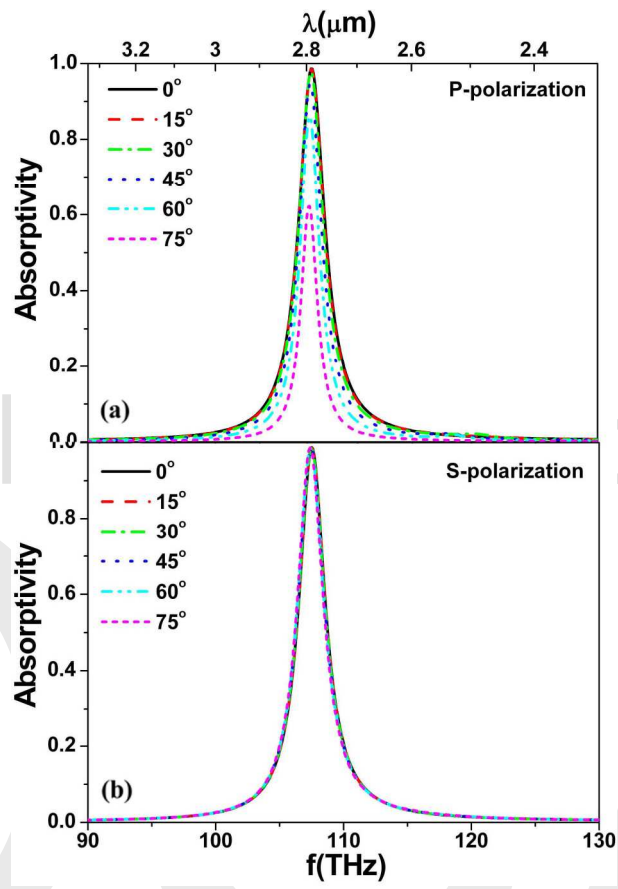


Fig 5